Theor Appl Genet (2006) 112: 373–381
DOI 10.1007/s00122-005-0140-y

ORIGINAL PAPER

Vamsi J. Nalam · M. Isabel Vales
Christy J. W. Watson · Shahryar F. Kianian
Oscar Riera-Lizarazu

Map-based analysis of genes affecting the brittle rachis character in tetraploid wheat (*Triticum turgidum* L.)

Received: 17 October 2005 / Accepted: 24 October 2005 / Published online: 19 November 2005

Abstract The mature spike rachis of wild emmer [*Triticum turgidum* L. ssp. *dicoccoides* (Körn. ex Asch. and Graebner) Thell.] disarticulates spontaneously between each spikelet leading to the dispersion of wedge-type diaspores. By contrast, the spike rachis of domesticated emmer (*Triticum turgidum* L. ssp. *turgidum*) fails to disarticulate and remains intact until it is harvested. This major distinguishing feature between wild and domesticated emmer is controlled by two major genes, *brittle rachis 2* (*Br-A2*) and *brittle rachis 3* (*Br-A3*) on the short arms of chromosomes 3A and 3B, respectively. Because of their biological and agricultural importance, a map-based analysis of these genes was undertaken. Using two recombinant inbred chromosome line (RICL) populations, *Br-A2*, on chromosome 3A, was localized to a ~11-cM region between *Xgwm2* and a cluster of linked loci (*Xgwm666.1, Xbarc19, Xcfa2164, Xbarc356*, and *Xgwm674*), whereas *Br-A3*, on chromosome 3B, was localized to a ~24-cM interval between *Xbarc218* and *Xwmc777*. Comparative mapping analyses suggested that both *Br-A2* and *Br-A3* were present in homoeologous regions on chromosomes 3A and 3B, respectively. Furthermore, *Br-A2* and *Br-A3* from wheat and *Btr1*/*Btr2* on chromosome 3H of barley (*Hordeum vulgare* L.) also were homoeologous suggesting that the location of major determinants of the brittle rachis trait in these species has been conserved. On the other hand, brittle rachis loci of wheat and barley, and a shattering locus on rice chromosome 1 did not appear to be orthologous. Linkage and deletion-based bin mapping comparisons suggested that *Br-A2* and *Br-A3* may reside in chromosomal areas where the estimated frequency of recombination was ~ 4.3 Mb/cM. These estimates indicated that the cloning of *Br-A2* and *Br-A3* using map-based methods would be extremely challenging.

Communicated by S. J. Knapp

V. J. Nalam · M. I. Vales · C. J. W. Watson
O. Riera-Lizarazu (✉)
Department of Crop and Soil Science, Oregon State University, 107 Crop Science Bldg, Corvallis, OR 97331, USA
E-mail: Oscar.Riera@oregonstate.edu
Tel.: +1-541-7375879
Fax: +1-541-7371589

S. F. Kianian
Department of Plant Sciences, North Dakota State University, Fargo, ND 58105, USA

Present address: V. J. Nalam
Department of Plant Pathology, Kansas State University, Manhattan, KS 66506, USA

Introduction

The brittle rachis of mature spikes of wild emmer wheat [*Triticum turgidum* L. ssp. *dicoccoides* (Körn. ex Asch. and Graebner) Thell.] disarticulates above the junction of the rachis and the point of spikelet insertion leading to the production of wedge-type diaspores (Zimmerman 1934). The mechanism of rachis disarticulation involves the development of an abscission or fracture zone at the joint of articulation of the spikelet and rachis (Zimmerman 1934; Matsumoto et al. 1963; Morrison 1994). This fracture zone collapses at maturity permitting the seed unit or spikelet to fall. The arrow-like morphology of the spikelets ensures that they passively penetrate surface litter and wedge themselves in cracks in the ground where they are safe from predation. In this context, the brittle rachis character is of evolutionary significance because of its adaptive value as an effective seed dispersal mechanism.

Unlike their wild progenitor, domesticated forms of emmer wheat [*T. turgidum* ssp. *dicoccum*, ssp. *turgidum*, ssp. *durum* (Desf.) Husnot, ssp. *polonicum* (L.) Thell., and ssp. *carthlicum* (Nevski in Kom.) Á. Löve and D. Löve] have a tough rachis where the formation of fracture zones is suppressed or the collapse of the rachis is delayed until mature spikes are collected or harvested. This feature resulted in the widespread adoption of cultivated tough-rachis emmer (*T. turgidum* ssp. *dicoccum*) during the Bronze Age (Bar-Yosef 1998). Thus,

selection of nonbrittle rachis mutants of emmer played a crucial role in the domestication of wheat in the Near East (for review see Salamini et al. 2002; Feldman 2001) that, in turn, enabled the emergence of early farming communities. In this context, the brittle rachis trait is tied to the origins of agriculture and sedentary societies.

Major spike characteristics that are relevant to the domestication of wheat such as spike shape, hulledness, and rachis brittleness were thought to be directly controlled by pleiotropic effects of a single factor, *Q* (Kuckuck 1964; Muramatsu 1986), that recently has been reported to be an *APETALA2*-like homeotic transcription factor (Faris et al. 2003). However, other researches have suggested that hulledness and rachis brittleness were primarily controlled by other loci (Luo et al. 2000). Various studies have shown that factors on homoeologous group 2 chromosomes directly affect hulledness and the free-threshing trait by controlling glume adherence or tenacity (Sears 1954; Kerber and Rowland 1974; Simonetti et al. 1999; Taenzler et al. 2002; Jantasuriyarat et al. 2004), whereas genes on homoeologous group 3 chromosomes primarily control rachis brittleness in wheat and other species of the Triticeae (Takahashi and Hayashi 1964; Riley et al. 1966; Urbano et al. 1988; Miller et al. 1995; King et al. 1997).

Due to the biological and agricultural importance of the brittle rachis trait, there have been a number studies aimed at understanding its genetic basis. Early experiments showed that the wedge-type disarticulation in *Triticum* was a dominant character (Love and Craig 1919). Cao et al. (1997) reported that rachis fragility of a feral or semi-wild wheat (*T. aestivum*) from Tibet was controlled by a single dominant gene, *brittle rachis 1* (*Br-A1*), that was later localized to the short arm of chromosome 3D by Chen et al. (1998). Similarly, Watanabe et al. (2002), using tetraploid wheat (*T. turgidum*) aneuploids, localized *brittle rachis 2* (*Br-A2*) and *brittle rachis 3* (*Br-A3*) to the short arms of chromosomes 3A and 3B, respectively. This was consistent with the assertion made by Feldman (2001) that the brittle rachis trait, in crosses between the bread wheat (*T. aestivum*) cultivar Bethlehem and the TTD140 accession of *T. turgidum* ssp. *dicoccoides* (Rong et al. 2000), was determined by dominant genes in the short arms of chromosomes 3A and 3B. Thus, genetic and cytogenetic analyses have consistently shown that the brittle rachis trait was controlled by loci on group 3 homoeologous chromosomes of both *T. aestivum* and *T. turgidum*. Besides these major determinants of the brittle rachis trait on chromosomes 3A, 3B, and 3D, loci on other chromosomes that modulate rachis fragility or regulate patterns of rachis disarticulation have also been described (Chen 2001).

Although the chromosome arm location of major genes that govern the brittle rachis trait in wheat had been determined, the localization of these factors with respect to a sparse number of DNA-based markers is fairly recent (Watanabe et al. 2005). Despite this new information, there are still questions concerning the organization and relationship between these loci. In order to clarify the relationship between *Br-A2* and *Br-A3* in *T. turgidum*, we carried out a project to place these genes on more comprehensive and denser linkage maps, and to determine the chromosome deletion bin location of these loci. In addition, map comparisons were performed to better understand the relationship among these loci; the relationship between these loci and a brittle rachis locus (*Btr1* and *Btr2*) in barley (*Hordeum vulgare* L.) (Takahashi and Hayashi 1964), and the relationship between brittle rachis loci and a shattering locus in rice (*Oryza sativa* L.) (Cai and Morishima 2000).

Materials and methods

Plant material

The localization of *brittle rachis 2* (*Br-A2*) and *brittle rachis 3* (*Br-A3*) and the development of linkage maps for chromosomes 3A and 3B were performed using two mapping populations. The mapping population for chromosome 3A (RICL-3A) consisted of 83 recombinant inbred chromosome lines (RICL) from a cross between Langdon (LDN) and the chromosome substitution line, LDN (*dicoccoides* 3A) [LDN(Dic-3A)] (Joppa 1993). Langdon is a *T. turgidum* ssp. *durum* cultivar, while LDN(Dic-3A) is a disomic chromosome substitution line that has the Langdon genetic background except for chromosome 3A which was derived from wild emmer (*T. turgidum* ssp. *dicoccoides*) (Joppa and Williams 1988). The mapping population for chromosome 3B (RICL-3B) consisted of 91 RICL lines developed from a cross between LDN and the LDN (*dicoccoides* 3B) [LDN (Dic-3B)] substitution line. The LDN(Dic-3B) substitution line has the Langdon genetic background except for chromosome 3B which was derived from wild emmer. Seeds for LDN, LDN(Dic-3A), LDN(Dic-3B), and the RICL populations (RICL-3A and RICL-3B) were kindly provided by Dr. Justin Faris (USDA-ARS, Fargo, North Dakota).

Cytogenetic stocks for homoeologous group 3 chromosomes were used to place markers to chromosomes and chromosome segments. These stocks included Chinese Spring nullisomic–tetrasomics (N3AT3B, N3AT3D, N3BT3A, N3BT3D, N3DT3A, and N3DT3B), ditelosomics (Dt3AS, Dt3AL, Dt3BS, and Dt3BL), four deletion lines for chromosome 3A (3AS-2, 3AS-4, 3AL-3, and 3AL-5), and five deletion lines for chromosome 3B (3BS-1, 3BS-8, 3BS-9, 3BL-1, 3BL-7). Deletion bin mapping and karyotype information for the chromosomes 3A and 3B deletion lines have been described in detail by Munkvold et al. (2004) and Qi et al. (2003). The Chinese Spring aneuploids were obtained from Dr. B. S. Gill (Kansas State University, Manhattan, KS, USA).

DNA isolation, microsatellite marker analysis, and mapping

About 30–50 mg of leaf tissue were used for DNA extraction. Plant tissue was ground using a Qiagen/Retsch MM300 mixer mill (Qiagen Inc, Valencia, CA, USA) and DNA was isolated as described by Riera-Lizarazu et al. (2000). Following DNA extraction, polymerase chain reaction (PCR) amplification of microsatellite markers was performed in a MWG Thermalcycler (Primus 96 Plus). Each PCR reaction was performed in a total volume of 10 µl containing 0.5 µM of each forward and reverse primer, 0.2 mM of each deoxynuleotide, 0.03 U/µl of *Taq* DNA Polymerase (Qiagen), 1× Taq buffer from Qiagen, 2% sucrose in 0.04% cresol red, and 50 ng of template DNA. The PCR amplification consisted of an initial denaturation step of 5 min at 94°C, followed by 45 cycles of three steps of 30 s each: denaturation at 94°C, annealing at 50, 55 or 60°C (depending on the individual marker), and extension at 72°C. A final extension step at 72°C for 10 min was performed, and the program ended holding it at 4°C. Products were electrophoresed in 4% (w/v) agarose gels and visualized after staining with ethidium bromide.

Markers (mostly microsatellites) from various sources previously mapped on chromosomes 3A and 3B were used (Nelson et al. 1995; Röder et al. 1998; Pestova et al. 2000; Somers et al. 2004; Yu et al. 2004; Song et al. 2005). Twenty-two polymorphic microsatellite loci were used for genetic mapping using the RICL-3A population. In addition, seven RFLP loci, previously mapped in this population (Otto et al. 2002), and morphological trait loci controlling the brittle rachis trait (*Br-A2*), and red grain color (*R-A1*) were mapped. The RICL-3B population was used to map brittle rachis (*Br-A3*) and grain color (*R-B1*) loci as well as 32 polymorphic microsatellite markers. Linkage maps for chromosomes 3A and 3B were constructed using JoinMap 3.0 (Van Ooijen and Voorrips 2001). Recombination fractions were converted into map distances (cM) using the Kosambi mapping function. Chromosome maps were drawn with MapChart 2.1 (Voorrips 2002).

Phenotypic assessments

The RICL-3A and RICL-3B populations were planted and grown to maturity at West Greenhouse, Oregon State University, in 2004. Before evaluation, mature spikes of plants from both RICL populations and their parents were dried at 54°C for 3 days. Subsequently, spikes with good seed fill were dropped from a height of 1.5 m. Spikes that disarticulated on impact were classified as brittle, and spikes that failed to disarticulate were classified as having a tough rachis. Three observers independently assessed the rachis fragility of different spikes in these populations. We also evaluated grain color since alleles of *R-A1* and *R-B1* were segregating in the RICL-3A and RICL-3B populations, respectively. The color of the grain (red or amber) from individuals of both populations was independently scored by two observers after seeds were soaked in a solution of 5% (w/v) NaOH for 1 h. Chi-square (χ^2) tests were performed to test the expected 1:1 segregation of brittle versus tough rachis, and red versus amber grain in both populations.

Results

The rachis of LDN was nonbrittle (Fig. 1a). On the other hand, the spikes of LDN(Dic-3A) and LDN(Dic-3B) were brittle and disarticulated with mechanical action (Fig. 1b, c). The spikes of LDN(Dic-3A) and LDN(Dic-3B) disarticulated at the node above the insertion point of the spikelet to the rachis creating a wedge-shaped spikelet attached to a subtending rachis internode (wedge-type diaspore). The pattern of disarticulation observed in LDN(Dic-3A) and LDN(Dic-3B) were similar to that observed in wild emmer, *T. turgidum* ssp. *dicoccoides*.

The segregation ratios of brittle to nonbrittle rachis in both RICL populations differed significantly from a 1 brittle:1 tough rachis ratio (Table 1). In both populations, there was an excess of individuals with a tough rachis. The segregation for grain color in the RICL-3B population did not significantly differ from the 1 red: 1 amber grain color ratio. On the other hand, the segregation for grain color in the RICL-3A population differed significantly from the expected ratio where an excess of red grain was observed (Table 1).

The linkage map of chromosome 3A contained 31 loci and spanned 155 cM (Fig. 2a). The average distance between markers in this linkage map was 7 cM. The largest interval in the map was 21 cM between *Xbarc294* and the linked markers, *Xbarc310* and *Xbarc12*, at the terminal end of the short arm of chromosome 3A. *Br-A2* was mapped to an 11-cM interval between *Xgwm2* and a cluster of linked loci (*Xgwm666.1, Xbarc19, Xcfa2164, Xbarc356*, and *Xgwm674*). The red grain locus *R-A1* and a linked marker, *Xwmc153*, was mapped to a 4-cM interval flanked by *Xcfa2193* and *Xbarc51* (Fig. 2a). *Br-A2* on the short arm of this chromosome showed significant ($P < 0.05$) segregation distortion with an excess of Langdon alleles. In the long arm, the interval composed of *Xcfa2193*, *R-A1*, and *Xwmc153* also showed significant ($P < 0.05$) distorted segregation ratios with an excess of LDN (Dic-3A) alleles (Fig. 2a). The length of this linkage map and the order of markers were comparable to comprehensive maps of chromosome 3A that include a sizeable number of microsatellite markers (Somers et al. 2004; Song et al. 2005). A notable anomaly in our map was the placement of *Xgwm666.2*, *Xcfa2076*, and *Xwmc169* with respect to the microsatellite consensus map reported by Somers et al. (2004).

The linkage map of chromosome 3B contained 35 loci and spanned 162 cM with an average distance between

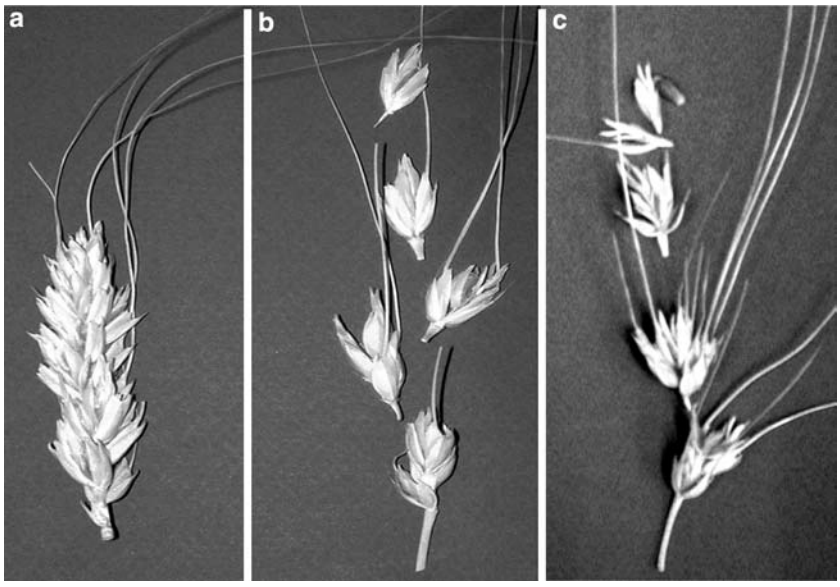

Fig. 1 Pattern of spike disarticulation of *Triticum turgidum* cv. Langdon (**a**) and the Langdon (Dic-3A) (**b**) and Langdon (Dic-3B) (**c**) disomic chromosome substitution lines

markers of 6 cM (Fig. 2c). The largest interval was a 22-cM region between *Xbarc218* and *Br-A3*. The brittle rachis locus, *Br-A3*, was localized to a 24-cM interval between *Xbarc218* and *Xwmc777*. The red grain locus in this map, *R-B1*, was mapped to a 10-cM interval flanked by *Xbarc84* and the linked markers *Xbarc229* and *Xwmc291* (Fig. 2c). In the short arm, markers in the *Br-A3–Xgwm264* interval showed significant ($P < 0.05$) segregation distortion. Similarly, markers in the *Xwmc1–Xwmc291* interval, near *R-B1*, also showed significant ($P < 0.05$) segregation distortion (Fig. 2c). In all cases, there was an excess of Langdon alleles. The length and order of this map was comparable to other published maps (Somers et al. 2004; Song et al. 2005). However, some anomalies included the placement of *Xwmc777*, *Xwmc527*, *Xwmc632*, and *Xgwm547* when compared to the consensus map reported by Somers et al. (2004).

Chinese Spring deletion stocks were used to place genetic loci into chromosomes bins on chromosomes 3A and 3B. Markers associated with *Br-A2* (*Xgwm2* and *Xbarc45*) on the short arm of chromosome 3A were placed in the most distal bin 3AS4-0.45-1.0 (Fig. 2b). We were not able to unambiguously place *Xgwm666.1* to a chromosomal bin because of its multi-copy nature, but Sourdille et al. (2004) suggested that this locus is also located in bin 3AS4-0.45-1.0. Other microsatellite loci such as *Xbarc356, Xbarc19, Xgwm674*, and *Xcfa2164* in the short arm of chromosome 3A were placed in deletion bin 3AS2-0.23-0.45 (Fig. 2b). Markers associated with *Br-A3* (*Xksum45, Xwmc43, Xbarc218, Xwmc777, Xwmc540*, and *Xgwm264*) on the short arm of chromosome 3B were placed into deletion bin 3BS1-0.33-0.57 (Fig. 2d).

Discussion

The brittle rachis trait in *T. turgidum* is governed by two dominant genes, *Br-A2* and *Br-A3*, present on the short arms of chromosomes 3A and 3B, respectively (Watanabe and Ikebata 2000; Watanabe et al. 2002). Recently, Watanabe et al. (2005) localized *Br-A2* to a 26-cM interval between *Xgwm779* and *Xgwm32*, whereas *Br-A3* was localized to a 47-cM interval flanked by *Xgwm685* and *Xgwm72*. *Br-A2* was ~13 cM from either

Table 1 Joint segregation for brittle rachis and grain color in the RICL-3A and RICL-3B populations

	Grain color	Rachis				Chi-square[b]
		Brittle	Tough	Missing[a]	Total	
RICL-3A	Red	18	33	1	52	5.31*
	Amber	12	19	0	31	
	Total	30	52	1	83	
	Chi-square[c]	5.90*				
RICL-3B	Red	18	18	1	37	3.18
	Amber	16	38	0	54	
	Total	34	56	1	91	
	Chi-square[c]	5.38*				

[a]Missing data points in the RICL-3A and RICL-3B populations
[b]Chi-square values testing for a 1:1 segregation of red versus amber grain color. *Significant deviation from the 1:1 ratio at $P < 0.05$
[c]Chi-square values testing for a 1:1 segregation of tough versus brittle rachis. *Significant deviation from the 1:1 ratio at $P < 0.05$

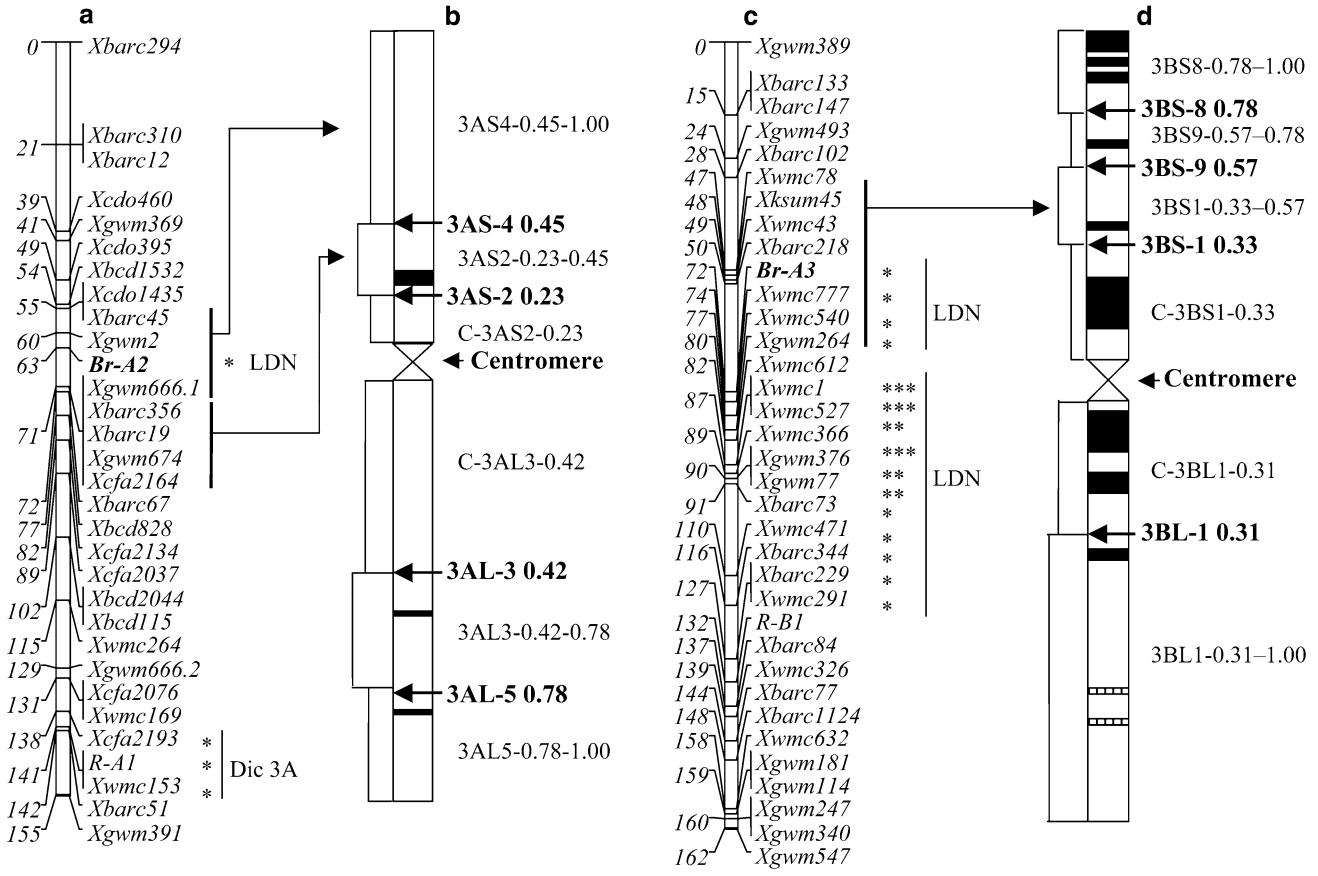

Fig. 2 Genetic linkage maps of chromosomes 3A and 3B showing the location of *Br-A2* and *Br-A3* and their relationship to chromosome deletion bins. **a** Genetic linkage maps of chromosomes 3A showing the location of *Br-A2* (*bold*). Genetic distances, on the *left*, are given in centiMorgans (cM, Kosambi). Marker names are given on the *right* side of each chromosome. Markers showing segregation distortion are indicated by * significant distortion at $P < 0.05$, and ** $P < 0.01$. The "LDN" abbreviation indicates markers exhibiting an excess of Langdon alleles, whereas the "Dic3A" abbreviation indicates markers exhibiting an excess of Langdon (Dic-3A) alleles. **b** Ideogram of C-banded chromosome 3A (Gill et al. 1991) with deletion breakpoints (based on Qi et al. 2003) indicated by *arrows*. **c** Genetic linkage map of chromosome 3B showing the location of *Br-A3* (*bold*). Markers showing segregation distortion are indicated by * significant distortion at $P < 0.05$, ** $P < 0.01$, and *** $P < 0.001$. The "LDN" abbreviation indicates markers exhibiting an excess of Langdon alleles. **d** Ideogram of C-banded chromosome 3B (Gill et al. 1991) with deletion breakpoints (based on Qi et al. 2003) indicated by *arrows*.

flanking marker (*Xgwm779* or *Xgwm32*), while *Br-A3* was ~14 cM from its closest marker (*Xgwm72*). In our study, *Br-A2* was localized to an 11-cM interval between *Xgwm2* and a cluster of linked loci (*Xgwm666.1, Xbarc19, Xcfa2164, Xbarc356*, and *Xgwm674*) on chromosome 3A, whereas *Br-A3* was localized to a 24-cM interval between *Xbarc218* and *Xwmc777* on chromosome 3B (Fig. 2a, c). The location of these loci was consistent with the report of Watanabe et al. (2005) and our use of a larger number of markers resulted in the identification of markers with tighter linkage to these genes—*Xgwm2* was found to be 3.3 cM from *Br-A2*, whereas *Xwmc777* was found to be 2.3 cM from *Br-A3*. A comparison between the linkage maps of chromosomes 3A and 3B from this study and other maps based on common microsatellite and RFLP markers (Nelson et al. 1995; Somers et al. 2004; Song et al. 2005) suggested that *Br-A2* and *Br-A3* mapped to homoeologous segments on these chromosomes (Fig. 3). Thus, our analysis provided strong support for the position of Watanabe et al (2002, 2005) that *Br-A2* and *Br-A3* were homoeologous.

Br-A2 was flanked by the RFLP marker loci *Xcdo1435* and *Xbcd828* on chromosome 3A (Fig. 2a). These and adjacent markers on the integrated and consensus maps of chromosome 3H of barley (*H. vulgare*) (Qi et al. 1996; Kleinhofs and Graner 2001) also flank two complementary linked loci, *Btr1*/*Btr2*, that control the brittle rachis trait (Takahashi and Hayashi 1964; Komatsuda and Mano 2002; Kandemir et al. 2004) (Fig. 3). Thus, map comparisons showed that *Br-A2* and *Br-A3* from wheat and *Btr1*/*Btr2* from barley were also

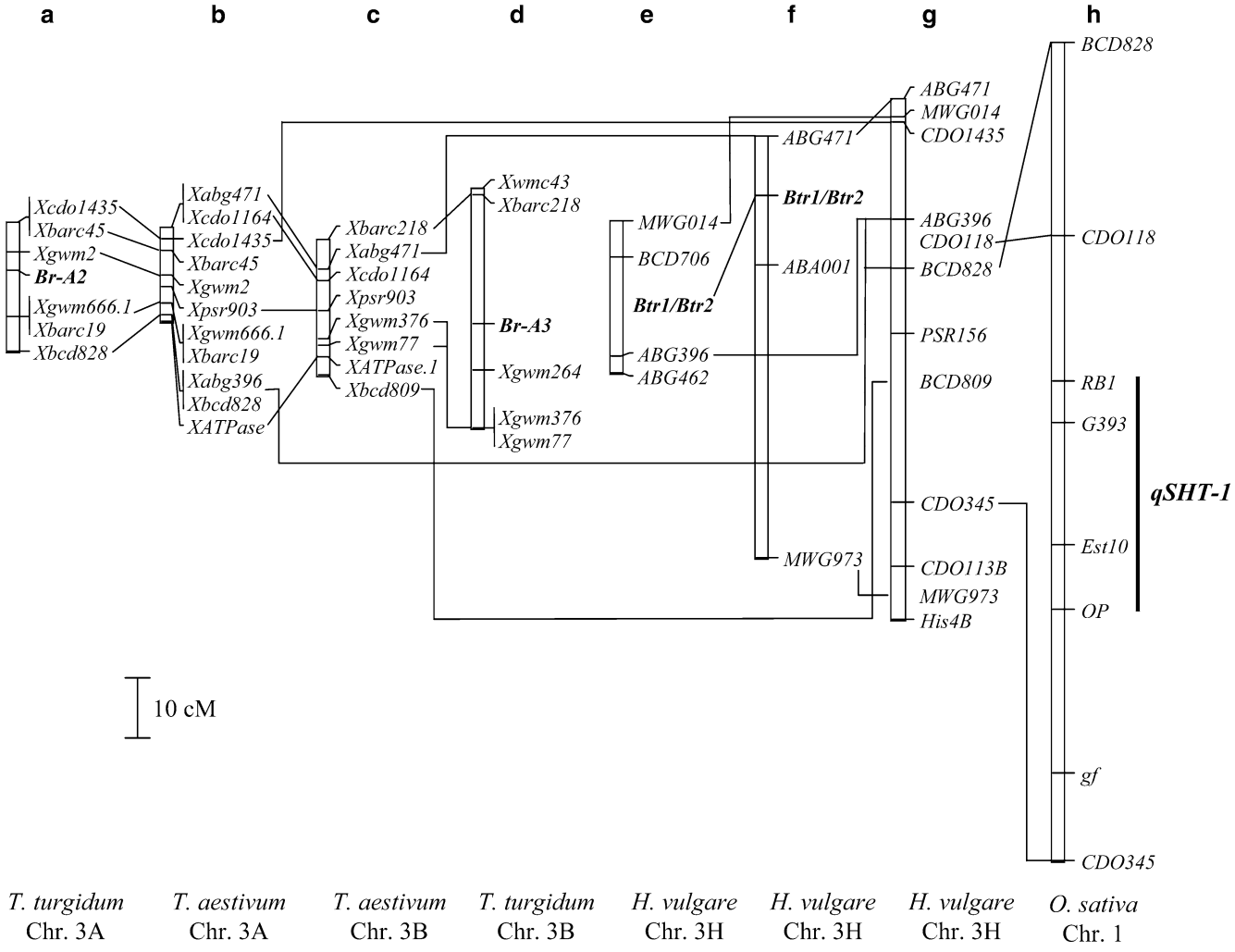

Fig. 3 Partial linkage maps of chromosomes 3A and 3B of wheat (*Triticum turgidum* and *T. aestivum*), chromosome 3H of barley (*Hordeum vulgare*) and chromosome 1 of rice (*Oryza sativa*) showing regions of conserved synteny with loci controlling the brittle rachis trait and shattering. The partial linkage maps of the short arms of chromosomes 3A (**a**) and 3B (**d**) of *T. turgidum* along with the locations of the brittle rachis loci, *Br-A2* and *Br-A3* (*bold*), respectively, are based on this study. The partial linkage maps of chromosomes 3A (**b**) and 3B (**c**) of *T. aestivum* were based on the report by Song et al. (2005). The partial linkage maps of chromosome 3H of *H. vulgare* were based on maps developed by Kandemir et al. (2004) (**e**) and Komatsu and Mano (2002) (**f**) both showing the location of two tightly linked brittle rachis loci, *Btr1*/*Btr2* (*bold*), and the integrated bin map (**g**) described by Kleinhofs and Graner (2001) (http://barleygenomics.wsu.edu). The partial linkage map of chromosome 1 (**h**) of *O. sativa* showing the approximate location of a quantitative trait locus (*QTL*) for seed shattering (*qSHT-1*) was based on Cai and Morishima (2000)

homoeologous suggesting that the locations of major determinants of the brittle rachis trait in these species have been conserved.

Since homoeologous group 3 chromosomes of the Triticeae have conserved synteny with rice chromosome 1 (Smilde et al. 2001; Sorrells et al. 2003; Munkvold et al. 2004), and rice chromosome 1 was known to contain genes/factors for shattering (Xiong et al. 1999; Cai and Morishima 2000), we performed map comparisons to assess the relationship between shattering loci in rice and brittle rachis loci in wheat. A quantitative trait locus or loci (QTL) on rice chromosome 1, that controls shattering, has been consistently detected in various populations (Xiong et al. 1999; Cai and Morishima, 2002, 2002; Zhang et al. 2002; Thomson et al. 2003) (Fig. 3). Furthermore, Cai and Morishima (2000) and Zhang et al. (2002) have suggested that QTL in this region of rice chromosome 1 represented the action of *sh2*, a major shattering gene known to regulate the formation of abscission zones in maturing rice panicles (Oba et al. 1990). Our comparative analyses (Fig. 3) showed that the rice shattering QTL (*qSHT-1*) reported by Cai and Morishima (2000, 2002) was located in a region on rice chromosome 1 that was syntenous with regions on chromosomes 3A, 3B, and 3H that were proximal to the locations of *Br-A2*, *Br-A3*, and *Btr1*/*Btr2*, respectively. Thus, *qSHT-1* and brittle rachis loci of wheat and barley did not appear to be orthologous. However, additional mapping with more common markers would be needed to permit a better assessment of the relationship among these loci since chromosomal rearrangements in syntenic regions have been observed (Sorrells et al. 2003) and

these can lead to discontinuities in the order of genetic loci.

Marker segregation distortion has been reported in intervarietal as well as interspecific crosses in wheat (Candalen et al. 1997). In our study, the segregation distortion in chromosome 3B was more severe to that observed in chromosome 3A (Fig. 2a, c). Except for the distorted region in the long arm chromosome 3A, segregation distortion was characterized by an excess of *T. turgidum* cv. Langdon alleles. Thus, we observed an excess of lines with a tough rachis (Langdon allele) in both the mapping populations (RICL-3A and RICL-3B) that we studied. Watanabe et al. (2002) determined that the brittle rachis trait in crosses between Langdon and LDN(Dic-3A), and between Langdon and LDN(Dic-3B) were due to single genetic factors in both cases. Since the region of segregation distortion around *Br-A3* (Fig. 2c) extended to nearby loci, segregation distortion in the RICL-3A and RICL-3B populations may be due to an unconscious selection of tough-rachis genotypes in the development of the RICL populations or selection of factors, near *Br-A2* and *Br-A3*, that affected gametophyte competitive ability (Faris et al. 1998). Segregation distortion was also observed in the long arms of chromosomes 3A and 3B near loci that affected grain color (Fig. 2a, c). Distortion on the long arm of chromosome 3B was due to an excess of Langdon alleles, whereas the distortion on chromosome 3A was due to an excess of LDN (Dic-3A) alleles. Thus, no specific pattern with respect to the source of the chromosome regions was evident. It is interesting to note that segregation distortion in comparable chromosomal regions has been observed elsewhere (Shah et al. 1999; Nachit et al. 2001; Paillard et al. 2003) suggesting that distortions may have a genetic basis. Nonetheless, additional investigations are needed to establish the nature of segregation distortion in these regions.

Using wheat deletion stocks we localized *Br-A2* to bin 3AS4-0.45-1.00 (Fig. 2b) since it was flanked by markers that reside in this bin. Similarly, *Br-A3* was placed in bin 3BS1-0.33-0.57 (Fig. 2d). The localization of microsatellite loci to chromosomal bins was consistent with the report of Sourdille et al. (2004). Due to the lack of common markers, the location of *Br-A2* and *Br-A3* with respect to consensus gene-rich regions (GRRs) by Erayman et al. (2004) could not be unequivocally determined. On the other hand, map comparisons showed that these genes were present in homoeologous regions that also contain homoeologous *Xpsr903* loci (Nelson et al. 1995; Song et al. 2005). Since *Xpsr903* has been localized to the homoeologous group 3 consensus 3S0.5 GRR, it is likely that *Br-A2* and *Br-A3* also reside in this GRR. The 3S0.5 GRR, delimited by the deletions 3DS-1(0.39) and 3BS-2(0.56), has an estimated physical size of 60 Mb and an estimated frequency of recombination of 4.3 Mb/cM (Erayman et al. 2004). These estimates indicate that cloning *Br-A2* and *Br-A3* using map-based methods would be extremely challenging since these genes may reside in relatively gene-poor chromosomal areas with moderate to low levels of recombination. In this regard, a thorough assessment of the relationship between brittle rachis loci of wheat and rice (*Oryza sativa* L.) should be explored to evaluate the possibility of using the substantial genomics resources in rice for a more targeted approach to the isolation of brittle rachis loci in wheat. Since the formation of abscission or fracture zones is a ubiquitous process in plants (Jarvis et al. 2003), that may have conserved regulation (Dinneny and Yanofsky 2005), developments in this area of research may also be helpful in the identification of candidate genes for the evolutionarily and agriculturally important brittle rachis loci in wheat.

Acknowledgements We thank Dr. Justin Faris and Dr. Bikram Gill for providing seed of the genetic stocks used in this study. We also thank Jason Nunes, Robin Treuer, Carla Otto, and Justin Hegstad for their technical assistance. Funding from the Oregon Agricultural Experiment Station is gratefully acknowledged.

References

Bar-Yosef O (1998) The Natufian Culture in the Levant, threshold of the origin of agriculture. Evol Anthropol 6:159–177

Cadalen T, Boeuf C, Bernard S, Bernard M (1997) An intervarietal molecular marker map in *Triticum aestivum* L. Em. Thell. and comparison with a map from a wide cross. Theor Appl Genet 94:367–377

Cai HW, Morishima H (2000) Genomic regions affecting seed shattering and seed dormancy in rice. Theor Appl Genet 100:840–846

Cai HW, Morishima H (2002) QTL clusters reflect character associations in wild and cultivated rice. Theor Appl Genet 104:1217–1228

Cao W, Scoles G J, Hucl P (1997) The genetics of rachis fragility and glume tenacity in semi-wild wheat. Euphytica 94:119–124

Chen Q-F (2001) Inheritance of disarticulation derived from some hexaploid brittle rachis wheat. Genet Res Crop Evol 48:21–25

Chen Q-F, Yen C, Yang J-L (1998) Chromosome location of the gene for brittle rachis in the Tibetan weedrace of common wheat. Genet Res Crop Evol 45:21–25

Dinneny JR, Yanofsky MF (2005) Drawing lines and borders: how the dehiscent fruit of *Arabidopsis* is patterned. Bioessays 27:42–49

Erayman M, Sandhu D, Sidhu D, Dilbirligi M, Baenziger PS, Gill KS (2004) Demarcating the gene-rich regions of the wheat genome. Nucleic Acids Res 32:3546–3565

Faris JD, Fellers JP, Brooks SA, Gill BS (2003) A bacterial artificial chromosome contig spanning the major domestication locus *Q* in wheat and identification of a candidate gene. Genetics 164:311–321

Faris JD, Laddomada B, Gill BS (1998) Molecular mapping of segregation distortion loci in *Aegilops tauschii*. Genetics 149:319–327

Feldman M (2001) Origin of cultivated wheat. In: Bonjean A P, Angus W J (eds) The world wheat book: a history of wheat breeding. Lavoisier, Paris, pp 3–56

Gill BS, Friebe B, Endo TR (1991) Standard karyotype and nomenclature system for description of chromosome bands and aberrations in wheat (*Triticum aestivum*). Genome 34:830–839

Jantasuriyarat C, Vales MI, Riera-Lizarazu O (2004) Identification and mapping of genetic loci affecting the free-threshing habit and spike compactness in wheat (*Triticum aestivum* L.). Theor Appl Genet 108:261–273

Jarvis MC, Briggs SPH, Knox JP (2003) Intercellular adhesion and cell separation in plants. Plant Cell Environ 26:977–989

Joppa LR (1993) Chromosome engineering in tetraploid wheat. Crop Sci 33:908–913
Joppa LR, Williams ND (1988) Langdon durum substitution lines and aneuploid analysis in tetraploid wheat. Genome 30:222–228
Kerber ER, Rowland GG (1974) Origin of the free threshing character in hexaploid wheat. Can J Genet Cytol 16:145–154
Kandemir N, Yildirim A, Kudrna DA, Hayes PM, Kleinhofs A (2004) Marker assisted genetic analysis of non-brittle rachis trait in barley. Hereditas 141:272–277
King IP, Law CN, Cant KA, Orford SE, Reader SM, Miller TE (1997) *Tritipyrum* a potential new salt-tolerant cereal. Plant Breed 116:127–132
Kleinhofs A, Graner A (2001) An integrated map of the barley genome. In: Phillips RL, Vasil IK (eds) DNA-based markers in plants, 2nd edn. Kluwer, Dordrecht, pp 187–199
Komatsuda T, Mano Y (2002). Molecular mapping of the intermedium spike-c (*int-c*) and non-brittle rachis 1 (*btr1*) loci in barley (*Hordeum vulgare* L). Theor Appl Genet 105:85–90
Kuckuck H (1964) Experimentelle Untersuchungen zur Entstehung der Kulturweizen. Z Pflanzenzuchtg 51:97–140
Love HH, Craig WT (1919) The synthetic production of wild wheat forms. J Hered 10:51–64
Luo MC, Yang ZL, Dvorak J (2000) The *Q* locus of Iranian and European spelt wheat. Theor Appl Genet 100:601–606
Matsumoto K, Teramura T, Tabushi J (1963) Development analysis of the rachis disarticulation in *Triticum*. Wheat Infor Serv 15–16:23–26
Miller TE, Reader SM, Mahmood A, Purdie KA, King IP (1995) Chromosome 3N of *Aegilops uniaristata*—a source of tolerance to high levels of aluminum for wheat. In: Li ZS, Xin ZY (eds) Proceedings of 8th international wheat genet symposium. China Agricultural Scientech Press, Beijing, China, pp 1037–1042
Morrison LA (1994) Reevaluation of systematic relationships in *Triticum* L. and *Aegilops* L. based on comparative morphological and anatomical investigations of dispersal mechanisms. PhD Thesis, Oregon State University
Muramatsu M (1986) The vulgare super gene, *Q*: its universality in durum wheat and its phenotypic effects in tetraploid and hexaploid wheats. Can J Genet Cytol 28:30–41
Munkvold JD, Greene RA, Bermudez-Kandianis CE, La Rota CM, Edwards H, Sorrells SF, Dake T, Benscher D, Kantety R, Linkiewicz AM, Dubcovsky J, Akhunov ED, Dvorak J, Miftahudin, Gustafson JP, Pathan MS, Nguyen HT, Matthews DE, Chao S, Lazo GR, Hummel DD, Anderson OD, Anderson JA, Gonzalez-Hernandez JL, Peng JH, Lapitan N, Qi LL, Echalier B, Gill BS, Hossain KG, Kalavacharla V, Kianian SF, Sandhu D, Erayman M, Gill KS, McGuire PE, Qualset CO, Sorrells ME (2004) Group 3 chromosome bin maps of wheat and their relationship to rice chromosome 1. Genetics 168:639–650
Nachit MM, Elouafi I, Pagnotta A, El Saleh A, Iacono E, Labhilili M, Asbati A, Azrak M, Hazzam H, Benscher D, Khairallah M, Ribaut J-M, Tanzarella OA, Porceddu E, Sorrells ME (2001) Molecular linkage map for an intraspecific recombinant inbred population of durum wheat (*Triticum turgidum* L var *durum*). Theor Appl Genet 102:177–186
Nelson JC, Van Deynze AE, Autrique E, Sorrells ME, Lu YH, Negre S, Bernard M, Leroy P (1995) Molecular mapping of wheat homoeologous group 3. Genome 38:525–533
Oba S, Kikuchi F, Maruyama K (1990) Genetic analysis of semidwarfness and grain shattering of Chinese rice variety "Ai-Jio-Nana-Te". Japan J Breed 40:13–20
Otto CD, Kianian SF, Elias EM, Stack RW, Joppa LR (2002) Genetic dissection of a major *Fusarium* head blight QTL in tetraploid wheat. Plant Mol Biol 48:625–632
Paillard S, Schnurbusch T, Winzeler M, Messmer M, Sourdille P, Abderhalden O, Keller B, Schachermayr G (2003) An integrative genetic linkage map of winter wheat (*Triticum aestivum* L.). Theor Appl Genet 107:1235–1242
Pestsova E, Ganal MW, Röder MS (2000) Isolation and mapping of microsatellite markers specific for the D genome of bread wheat. Genome 43:689–697
Qi L, Echalier B, Friebe B, Gill BS (2003) Molecular characterization of a set of wheat deletion stocks for use in chromosome bin mapping of ESTs. Funct Integr Genomics 3:39–55
Qi X, Stam P, Lindhout P (1996) Comparison and integration of four barley genetic maps. Genome 39:379–394
Riera-Lizarazu O, Vales MI, Ananiev EV, Rines HW, Phillips RL (2000) Production and characterization of maize chromosome 9 radiation hybrids derived from an oat–maize addition line. Genetics 156:327–339
Riley R G, Kumber G, Law CN (1966) Correspondence between wheat and alien chromosomes. Ann Rep Plant Breed Inst 1964–65:108–109
Röder MS, Korzun V, Wendehake K, Plaschke J, Tixier MH, Leroy P, Ganal MW (1998) A microsatellite map of wheat. Genetics 149:2007–2023
Rong JK, Millet E, Manisterski J, Feldman M (2000) A new powdery mildew resistance gene: introgression from wild emmer into common wheat and RFLP-based mapping. Euphytica 115:121–126
Salamini F, Özkan H, Brandolini A, Schäfer-Pregl R, Martin W (2002) Genetics and geography of wild cereal domestication in the Near East. Nat Rev Genet 3:429–441
Sears ER (1954) The aneuploids of common wheat. University of Missouri, Columbia, pp 3–58
Shah MM, Gill KS, Baenziger PS, Yen Y, Kaeppler SM, Ariyarathne HM (1999) Molecular mapping of loci for agronomic traits on chromosome 3A of bread wheat. Crop Sci 39:1728–1732
Simonetti MC, Bellomo MP, Laghetti G, Perrino P, Simeone R, Blanco A (1999) Quantitative trait loci influencing free-threshing habit in tetraploid wheats. Genet Res Crop Evol 46:267–271
Smilde WD, Haluśkova J, Sasaki T, Graner A (2001) New evidence for the synteny of rice chromosome 1 and barley chromosome 3H from rice expressed sequence tags. Genome 44:361–467
Somers DJ, Issac P, Edwards K (2004) A high-density microsatellite consensus map for bread wheat (*Triticum aestivum* L.). Theor Appl Genet 109:1105–1114
Song QJ, Shi JR, Singh S, Fickus EW, Costa JM, Lewis J, Gill BS, Ward R, Cregan PB (2005) Development and mapping of microsatellite (SSR) markers in wheat. Theor Appl Genet 110:550–560
Sorrells ME, La Rota M, Bermudez-Kandianis CE, Greene RA, Kantety R, Munkvold JD, Miftahudin, Mahmoud A, Ma X, Gustafson JP, Qi LL, Echalier B, Gill BS, Matthews DE, Lazo GR, Chao S, Anderson OD, Edwards H, Linkiewicz AM, Dubcovsky J, Akhunov ED, Dvorak J, Zhang D, Nguyen HT, Peng J, Lapitan NL, Gonzalez-Hernandez JL, Anderson JA, Hossain K, Kalavacharla V, Kianian SF, Choi DW, Close TJ, Dilbirligi M, Gill KS, Steber C, Walker-Simmons MK, McGuire PE, Qualset CO (2003) Comparative DNA sequence analysis of wheat and rice genomes. Genome Res 13:1818–1827
Sourdille P, Singh S, Cadalen T, Brown-Guedira GL, Gay G, Qi L, Gill BS, Dufour P, Murigneux A, Bernard M (2004) Microsatellite-based deletion bin system for the establishment of genetic-physical map relationships in wheat (*Triticum aestivum* L.). Funct Integr Genomics 4:12–25
Taenzler B, Esposti RF, Vaccino P, Brandolini A, Effgen S, Heun M, Schafer-Pregl R, Borghi B, Salamini F (2002) Molecular linkage map of Einkorn wheat: mapping of storage-protein and soft-glum genes and bread-making quality QTLs. Genet Res Camb 80:131–143
Takahashi R, Hayashi J (1964) Linkage study of two complementary genes for brittle rachis in barley. Ber Ohara Inst Landw Biol Okayama Univ 12:99–105
Thomson MJ, Tai TH, McClung AM, Lai X-H, Hinga ME, Lobos KB, Xu Y, Martinez CP, McCouch SR (2003) Mapping quantitative trait loci for yield, yield components and morphological traits in an advanced backcross population between *Oryza rufipogon* and the *Oryza sativa* cultivar Jefferson. Theor Appl Genet 107:479–493

Urbano M, Rest P, Benedettelli S, Blanco A (1988) A *Dasypyrum villosum* (L.) Candargy chromosome related to homoeologous group 3 of wheat. In: Miller TE, Koebner RMD (eds) Proceedings of the 7th international wheat genetics symposium. IPSR Cambridge Lab, Cambridge, pp 169–173

Van Ooijen JW, Voorrips RE (2001) JoinMap 3.0, software for the calculation of genetic linkage maps. Plant Research International, Wageningen

Voorrips RE (2002) MapChart: software for the graphical presentation of linkage maps and QTLs. J Hered 93:77–78

Watanabe N, Ikebata N (2000) The effects of homoeologous group 3 chromosomes on grain color dependent seed dormancy and brittle rachis in tetraploid wheat. Euphytica 115:215–220

Watanabe N, Sugiyama K, Yamagashi Y, Sakata Y (2002) Comparative telosomic mapping of homoeologous genes for brittle rachis in tetraploid and hexaploid wheats. Hereditas 137:180–185

Watanabe N, Takesada N, Fujii Y, Martinek P (2005) Comparative mapping of genes for brittle rachis in *Triticum* and *Aegilops* (2005) Czech J Genet Plant Breed 41:39–44

Yu JK, Dake TM, Singh S, Benscher D, Li W, Gill B, Sorrells ME (2004) Development and mapping of EST-derived simple sequence repeat markers for hexaploid wheat. Genome 47:805–818

Xiong LZ, Liu KD, Dai XK, Xu CG, Zhang Q (1999) Identification of genetic factors controlling domestication-related traits of rice using a F_2 population of a cross between *Oryza sativa* and *O. rufipogon*. Theor Appl Genet 98:243–251

Zhang Z, Li P, Wang L, Tan C, Hu Z, Zhu Y, Zhu L (2002) Identification of quantitative trait loci (QTLs) for the characters of vascular bundles in peduncle related to indica-japonica differentiation in rice (*Oryza sativa* L.). Euphytica 128:279–284

Zimmerman JG (1934) Anatomische und morphologische Untersuchungen über die Brüchigkeit der Ahrenspindel in der Gattung *Triticum*. Z Zücht Reihe A Pflanzenzücht 19:164–182